JOURNAL OF MATERIALS SCIENCE 22 (1987) 3717–3720

Oxygen distribution in silicon nitride powders

MARCELL PEUCKERT
Hoechst AG, Keramikforschung G 864, Postfach 800320, D-6230 Frankfurt 80, FGR
PETER GREIL
Max-Planck-Institut für Metallforschung, Institut für Werkstoffwissenschaften, Pulvermetallurgisches Laboratorium, Heisenbergstrasse 5, D-7000 Stuttgart 80, FGR

The oxygen content of ten different silicon nitride powders was determined by bulk chemical analysis and surface-sensitive X-ray photoemission spectroscopy (XPS). In silicon nitride powders prepared from silicon and silica by nitridation and carbothermal reduction in a nitrogen atmosphere, respectively, only a minor part of the total oxygen content of 0.9 to 2.5 wt% was found in a surface layer of less than 1 nm thick, whereas an appreciable amount can be attributed to oxygen dissolved in the bulk. Powders made by silicon diimide decomposition, however, are characterized by a higher oxygen concentration at the particle surface relative to the bulk, which may be further reduced by chemical treatment. The surface layer composition corresponds to an intermediate state between silica and silicon oxynitride.

1. Introduction

Silicon nitride powders of high purity, small and homogeneous grain size are being developed for pressureless sintering of high-temperature resistant silicon nitride ceramics. These powders are mainly produced by nitridation of fine silicon powder, carbothermal reduction of silica and subsequent nitridation, gas-phase reaction of silanes with ammonia and thermal decomposition of silicon diimide [1–3]. Because of the higher free energy of formation of silica, silicon nitride will always be oxidized to silica or silicon oxynitride in the presence of an oxygen or water-containing atmosphere even though the reaction kinetics will be extremely slow at room temperature [4]. Thus the particle surfaces of silicon nitride powders are expected to be covered with an oxide-rich layer, which dominates the interparticle interactions and hence the powder properties such as agglomeration or dispersion in colloidal systems.

Various techniques have been used to characterize the structure and composition of the powder particle surfaces such as TEM, XPS and SIMS [5]. From the results a typical thickness of the oxide layer on several commercial silicon nitride powders of ~3 to 5 nm was deduced, with a composition corresponding to silicon oxynitride rather than to silica. From controlled oxidation experiments of clean silicon nitride films, the results of XPS also showed the oxidized layer having the composition of a "graded" oxynitride layer, with the elemental concentration of oxygen decreasing steadily with distance from the surface [6].

In contrast to the oxygen on the particle surface, only little information has yet been reported concerning the oxygen solubility in the bulk of silicon nitride powders. Previously, α-Si_3N_4 was considered to be an oxygen-stabilized silicon nitride modification with a composition of $Si_{23}N_{30}O$ [7, 8]. Subsequent investigations, however, proved the α-modification to be stable also in the total absence of oxygen [9]. Nevertheless, α-Si_3N_4, which is the predominant phase modification in commercial silicon nitride powders, is supposed to dissolve a certain amount of oxygen whereas no significant oxygen solubility in β-Si_3N_4 has yet been reported. While the dissolution of oxygen in pure silicon nitride is associated with the lattice defect structure, it is significantly enhanced by solid solution formation in the presence of certain metal atoms such as aluminium, magnesium, calcium, yttrium, etc. [10].

This study deals with the analysis of the distribution of oxygen in various commercial silicon nitride powders, which were produced by different methods. Surface-sensitive X-ray photoemission spectroscopy (XPS) and chemical analysis of the total oxygen content are applied to characterize the oxygen distribution in these powders.

2. Experimental procedure

2.1. Powders

Ten commercial silicon nitride powders were examined for their oxygen content: Anzon grade 1001, Warwick, GB (denoted A), Denka 9-FW, Tokyo, Japan (B), Kema Nord P-95, Ljungaverk, Sweden (C), H. C. Starck H-1, Berlin, FRG (D), H. C. Starck LC-10, Berlin, FRG (E), H. C. Starck LC-12, Berlin, FRG (F), Sumitomo Chem. TC-2, Osaka, Japan (G), Toshiba Grade A, Tokyo, Japan (H), Toyo Soda TS-7, Tokyo, Japan (I) and UBE E-10, Tokyo, Japan (K). Six of them, powders A to F, were produced by nitridation of metallic silicon, two by carbothermal reduction of silica in a nitrogen atmosphere, powders G and H, and two by thermal decomposition of silicon diimide, powders I and K.

2.2. Preparation of Si_2N_2O

Crystalline Si_2N_2O was prepared as a reference material by hot pressing a eutectic composition of α-Si_3N_4

0022–2461/87 $03.00 + .12 © *1987 Chapman and Hall Ltd.*

TABLE I XPS electron binding energies (eV)

	Si 2p	O 1s	N 1s
Si_3N_4 powders	101.1 ± 0.2	532.8 ± 0.2	397.5 ± 0.2
Si_2N_2O*	102.1	532.4	298.2
SiO_2†			
(cristobalite)	103.1 to	532.3 to	
(silica gel)	103.4	532.7	

*Hot-pressed specimen from [11].
†According to [13].

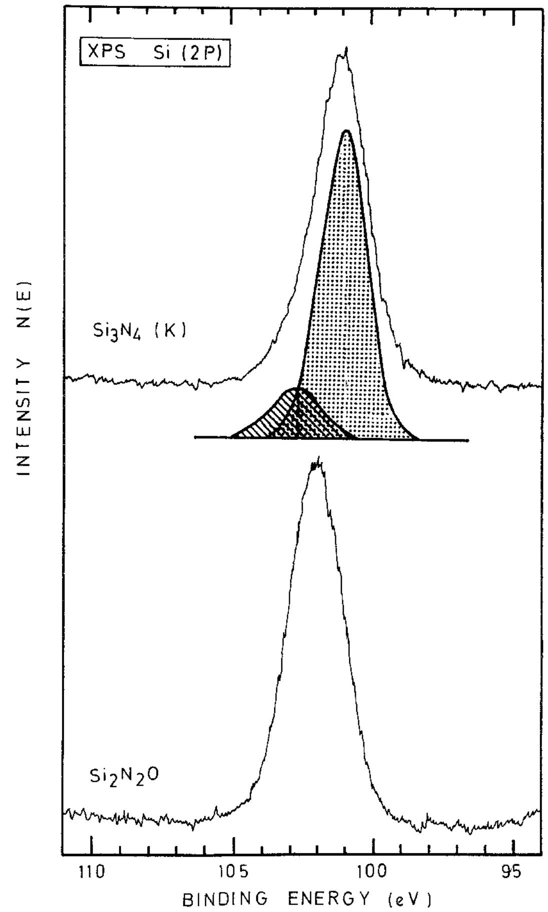

Figure 1 X-ray photoemission spectra of the Si 2p level for Si_3N_4 powder (K) and a hot-pressed Si_2N_2O sample [11]. The powder spectrum is deconvoluted into two peaks of equal half-width with an intensity ratio of 6.2 to 1 and electron binding energies of 101.1 and 102.8 eV, respectively.

and SiO_2 with 3 mol % Al_2O_3 at 1750° C with 35 MPa for 45 min [11]. XRD proved complete reaction to Si_2N_2O.

2.3. Bulk analysis

The total oxygen content of the powders was analysed by the inert gas fusion technique [12]. 20 to 30 mg dried powder was decomposed in liquid platinum at 2400° C in a graphite die in high vacuum. The oxygen was detected as CO by the change of the heat conductivity. The standard deviation of the mean value was approximately 5%.

2.4. Surface analysis

The specific surface area of the powders was measured by the BET method. Equivalent grain sizes assuming spherical grain morphology were deduced from these data and were used for calculation of an equivalent thickness of the surface oxide layers.

X-ray photoelectron spectra (XPS) were obtained with a Leybold-Heraeus LHS-10 system with a hemispherical energy analyser. A base pressure of 10^{-6} Pa was maintained during the analyses. Spectra were measured with a Mg$K\alpha$ X-ray source (1253.6 eV) and at a constant pass energy of 50 eV. Binding energies were referenced to the C1s peak at 284.6 eV which derives from the ubiquitous carbon contamination and the Scotch tape on to which the powder samples were fixed. For quantitative evaluation of the integrated peak areas (over a tangential baseline) atomic sensitivity factors of 0.63 for the O 1s and 0.38 for the N 1s level were used. These factors have previously been found to correspond well with the transmission function of our spectrometer [13, 14].

3. Results and discussion

3.1. X-ray photoelectron spectra

X-ray photoemission spectra were taken from all the Si_3N_4 powder samples A to K. The O 1s, N 1s and Si 2p signals were, in all cases, rather narrow and at almost identical binding energy levels for the different powders (Table I). The O 1s and N 1s peaks gave no evidence for more than one oxygen or nitrogen species. This is in contrast to previous measurements [5] where at least two different oxygen peaks where found. That at lower binding energy (529.7 eV) was attributed to oxidic oxygen bound to metallic impurities on the surface, e.g. iron oxide. Such a species was not observed in our study. The Si 2p signals were measured at 101.1 eV binding energy and those powders with a higher oxygen content or a thicker oxide layer also showed a weak shoulder at the high E_B side of the main peak (Fig. 1). In Table I the Si 2p, O 1s, and N 1s values are compared with literature data of various types of SiO_2 [15] and data obtained from a bulk Si_2N_2O sample [11]. The binding energies of the N 1s and the main Si 2p level can be regarded as typical of bulk Si_3N_4 and Si_2N_2O and they reflect the different modes of charge distribution in the compounds [5, 16, 17]. The O 1s level at 532.8 eV of the superficial oxidation layer on Si_3N_4 is slightly higher than that of Si_2N_2O and close to amorphous silica gel or vycor glass [15]. Deconvolution of the Si 2p spectrum of Si_3N_4 powder K (Fig. 1) revealed a small peak of about 102.8 eV binding energy which lies in between Si_2N_2O and SiO_2. Therefore, a clear identification of the surface layer as SiO_2 or Si_2N_2O cannot be made. An interpretation of our data in terms of a non-stoichiometric and, perhaps, amorphous oxynitride with a higher oxygen content than in crystalline Si_2N_2O seems more likely [16]. Also, a continuously changing or even layered structure could be in accord with our spectra [5].

3.2. XPS-derived oxide-layer thickness, d_{XPS}

From the relative O 1s and N 1s peak intensities it should be possible to calculate an equivalent thickness of the surface oxide layer assuming an ordered structure of a SiO_2 layer on the surface of the Si_3N_4 grains. The results obtained with such an idealized model do not vary significantly from results one would obtain with a more complex layer structure for which, on the other hand, no unequivocal evidence could be found. For the calculation, the peak intensities were corrected by atomic sensitivity factors (see Section 2) and average escape depths of $m = 1.2\,\text{nm}$ for the photoemission electrons (700 to 900 eV kinetic energy) were assumed. Because the intensity I_O of the O 1s peak is given by

$$I_O = I_O^0[I - \exp(-d/m)], \tag{1}$$

and the intensity I_N of the N 1s peak is given by

$$I_N = I_N^0 \exp(-d/m). \tag{2}$$

Assuming a layered particle surface structure model [14], the oxide layer thickness, d, can be derived from the ratio

$$\frac{I_O}{I_N} = \frac{I_O^0 (I - \exp(-d/m)]}{I_N^0 \exp(-d/m)} = \frac{I_O^0}{I_N^0 \exp(-d/m)} - \frac{I_O^0}{I_N^0} \tag{3}$$

such that

$$d_{XPS} = m \ln\left(\frac{I_O I_N^0}{I_N I_O^0} + 1\right) \tag{4}$$

where I_O and I_N are the measured O 1s and N 1s signal intensities and I_O^0 and I_N^0 are the theoretical XPS signal intensities that could be found with pure SiO_2 or Si_3N_4, respectively. The ratio I_N^0/I_O^0 is determined only by the relative atomic concentrations of nitrogen in Si_3N_4 and oxygen in SiO_2 [14], and a value of 1.03 was calculated.

Hence Equation 4 only holds under the simplifying assumption of a well-ordered layer structure of SiO_2 on the Si_3N_4 particle. Although earlier results have not shown a distinct oxide–nitride phase boundary but an oxynitride surface layer of various oxygen content [6], only a slightly larger thickness will be calculated when an oxynitride stoichiometry of the surface layer is assumed.

The equivalent surface layer thicknesses, d_{XPS}, as derived from Equation 4 are summarized in Table II. The thickness varies from 0.1 nm for powder B to 0.7 nm for powder G with an average value of 0.42 nm. The majority of the powders except powders B, D and F, reveal an oxide-rich layer thickness which corresponds only to one to two monolayers of silica with a SiO_4-tetrahedron size of ~0.265 nm.

TABLE II Comparison of surface and bulk oxygen analyses

Powder	S_v ($m^2 g^{-1}$)	C_O^t (wt %)	d_s (nm)	d_{XPS} (nm)	Fraction of surface oxygen (%)
A	7.3	1.4	1.6	0.4	25
B	12	0.9	0.6	0.1	17
C	8.8	1.3	1.2	0.7	58
D	10	1.4	1.2	0.2	17
E	15	1.5	0.9	0.4	44
F	21	1.3	0.5	0.14	28
G	15	2.4	1.4	0.7	51
H	10	2.5	2.1	0.5	24
I	12	1.4	1.0	0.6	60
K	12	0.9	0.6	0.5	83

The surface of powders B, D and F with $d_{XPS} < 0.2\,\text{nm}$ might then be described as a layer of adsorbed oxygen rather than a consistent oxide or oxynitride film. The Si 2p signals also give no evidence for thicker oxidation layers and only powders with $d_{XPS} > 0.4\,\text{nm}$ reveal a weak shoulder of the photoelectron peak at 102.8 eV due to enhanced Si–O bonding.

3.3. Surface and bulk oxygen

Table II also summarizes the results of specific surface area measurements by the BET-method and the total oxygen content of the silicon nitride powders as determined by chemical analysis. Using the specific surface area, S_v, an equivalent spherical particle diameter, D_s, can be calculated from the volume to surface ratio, v/s, of a sphere

$$D_s = 6\frac{v}{s} = \frac{6}{\varrho_{SN} S_v} = \frac{1.887 \times 10^{-6}}{S_v} \tag{5}$$

where ϱ_{SN} is the density of the material, i.e. $3.18 \times 10^6\,\text{g}\,\text{m}^{-3}$ in the case of $\alpha\text{-}Si_3N_4$.

If the total oxygen content of the powder, C_O^t was completely concentrated in a thin skin of SiO_2 on the surface of spherical particles, a fictive surface layer thickness, d_s, could be calculated as follows: the volume of the SiO_2 layer can be expressed as the difference between the total volume of the sphere with radius r_t and the volume of an unoxidized inner Si_3N_4 core of radius r_i

$$\tfrac{4}{3}\pi(r_t^3 - r_i^3) = \tfrac{4}{3}\pi r_t^3 \frac{\varrho_{SN} K C_O^t}{\varrho_{SO} 100} \tag{6}$$

ϱ_{SN}, ϱ_{SO}, and K are the densities of $\alpha\text{-}Si_3N_4$, SiO_2 (cristobalite), and a factor to convert wt % oxygen to wt % SiO_2, respectively.

Equation [6] is then transformed into

$$r_i = (1 - 0.02C_O^t)^{1/3} r_t \tag{7}$$

and the thickness, d_s, of the surface oxide layer is given by

$$d_s = r_t - r_i = [1-(1 - 0.026C_O^t)^{1/3}]r_t = [1-(1 - 0.026C_O^t)^{1/3}]\frac{D_s}{2} \tag{8}$$

The fictive oxide layer thicknesses, d_s, were calculated for powders A to K using Equations 5 and 8 and the values are listed in Table II. Assumption of larger particle sizes, D_s, as obtained by electron microscopy or sedimentation analysis, leads to larger thicknesses d_s according to Equation 8. These two methods, however, do not take into account the particle shape and, therefore, D_s values derived from surface-area measurements seem more appropriate for a comparison with XPS data, because the latter technique also probes the total powder surface area.

Comparison of d_s with d_{XPS} values clearly shows a consistent discrepancy between the results from both methods: the d_{XPS} are always less than the oxidation layer thickness, d_s, calculated from the total oxygen content of the powders. Because for both models an identical SiO_2 layer structure for the surface was assumed, this discrepancy can only be explained by a distribution of oxygen on the particle surface and in the bulk. The ratio of the total oxygen content which is concentrated on the particle was then derived from the d_{XPS}/d_s ratio and is given in the last column of Table II. Obviously, the powders made by silicon diimide decomposition, I and K, have concentrated most of the total oxygen content on their surface, 0.8 to 0.9 wt %, whereas only a very small amount of less than 0.15 wt % (powder K) can be attributed to oxygen dissolved in the α-Si_3N_4 crystal lattice. Powders A to F, which were made by nitridation of silicon, also show a very low amount of total oxygen but in general, except powder C, have more oxygen in the bulk, 0.6 to 1.1 wt %, than on the surface, 0.1 to 0.7 wt %. Finally, powders G and H, which were produced by carbothermal reduction of silica in a nitrogen atmosphere, are characterized by the highest amount of total oxygen of which 1.2 to 1.9 wt % are attributed to the bulk and 0.6 to 1.2 wt % to the surface. Some residual silica or silicon oxynitride may have resulted in the higher oxygen content of these powders.

From these results, an oxygen solubility in α-Si_3N_4 of approximately 0.8 ± 0.2 wt % at 1400° C is concluded. Earlier results corresponded to a solubility of 1.4 wt %, which was derived from an oxygen stabilized α-$Si_{23}N_{30}O$ composition [7, 8]. Surface and bulk oxygen of the powders, however, has not been distinguished.

3.4. Oxygen control in the powders

The oxygen-rich surface layer is probably produced by oxidation of the ultrafine powders, when they are exposed to an oxygen or water-containing atmosphere. Low temperature and oxygen/water-free storage are required to avoid uncontrolled surface oxidation during manufacturing and powder processing.

Only the surface-bonded oxygen will be sensitive to chemical purification treatment of the powders. Leaching in anhydrous hydrofluoric acid or treatment in flowing gas mixture of argon/hydrogen at 1300° C, has successfully been used to reduce the oxygen content of silicon nitride powders [5]. Although the chemical treatment was effective in reducing the oxygen content, a residual oxygen content of approximately 1 wt % always remained. This minimum oxygen content corresponds well to the oxygen solubility as derived by the authors.

While the surface-bonded oxygen can be manipulated by surface active treatment, dissolved oxygen in the bulk can hardly be reduced after powder synthesis. For this reason further improvement of sinterable silicon nitride powders will also be focused on the reduction of dissolved oxygen in the bulk. Purified raw materials containing only a minimum amount of oxygen gettering impurities such as aluminium, magnesium, calcium, etc., are supposed to be of particular significance as well as low reaction temperatures during powder synthesis.

4. Conclusions

The oxygen distribution in silicon nitride powders was investigated by bulk chemical analysis and surface sensitive XPS measurements. The majority of the powders, except the powders made by decomposition of silicon diimide, still contain an appreciable amount of oxygen in the bulk, from which an oxygen solubility of approximately 0.8 wt % was concluded.

A silica/silicon oxynitride composition is concluded for the particle surface layers, which were less than 1 nm thick. Chemical treatment can only reduce the surface-bonded oxygen content, while the dissolved oxygen remains in the bulk. The distribution of the oxygen contamination in a silicon nitride particle depends on the specific powder preparation method. Low-temperature synthesized silicon nitride powders from specifically purified materials are supposed to yield little oxygen in the bulk with a controlled oxygen distribution.

Acknowledgements

The authors wish to thank B. Bock, Dr W. Herzog, Dr H. J. Ostmann, and P. Papadopoulos for their technical assistance and helpful discussions. The Federal Ministry of Science and Technology (BMFT) is thanked for financial support.

References

1. D. R. GLASSON and S. A. A. JAYAWEERA, *J. Appl. Chem.* **18** (1968) 65.
2. K. S. MAZDIYASNI and L. M. COOKE, *J. Amer. Ceram. Soc.* **56** (1973) 628.
3. K. KOMEYA and H. INOUE, *J. Mater. Sci.* **10** (1975) 1244.
4. S. C. SINGHAL, *Ceram. Int.* **2** (1976) 123.
5. M. N. RAHAMAN, Y. BOITEUX and L. C. DEJONGHE, *Ceram. Bull.* **65** (1986) 1171.
6. S. I. RAIDER, R. FLITSCH, J. A. ABOOF and W. A. PLISKEN, *J. Electrochem. Soc.* **123** (1976) 560.
7. S. WILD, P. GRIEVENSON and K. H. JACK, *Spec. Ceram.* **5** (1972) 385.
8. H. FELD, P. ETTMAYER and I. PETZENHAUSER, *Ber. Dt. Keram. Ges.* **51** (1974) 127.
9. K. KATO, Z. INOUE, K. KIJIMA, I. KAWADA, H. TANAKA and T. YAMANE, *J. Amer. Ceram. Soc.* **58** (1975) 90.
10. J. WEISS, *Ann. Rev. Mater. Sci.* **11** (1981) 381.
11. Z. K. HUANG, P. GREIL and G. PETZOW, *Ceram. Int.* **10** (1984) 14.
12. J. MANGELS, *J. Mater. Sci.* **15** (1980) 2132.
13. G. E. MUILENBERG (ed.), "Handbook of X-Ray Photoelectron Spectroscopy" (Perkin Elmer, Physical Electronics Division, Eden Prairie, Minnesota, 1979).
14. M. PEUCKERT and H. P. BONZEL, *Surface Sci.* **145** (1984) 239.
15. C. D. WAGNER, D. E. PASSOJA, H. F. HILLERY, T. G. KINSKY, H. A. SIX, W. T. JANSEN and J. A. TASYLOR, *J. Vac. Sci. Technol.* **21** (1982) 933.
16. R. K. BROW and C. G. PANTANO, *J. Amer. Ceram. Soc.* **69** (1986) 314.
17. W. BRAUE, H. J. DUDEK and G. ZIEGLER, *J. Non-Cryst. Solids* **56** (1983) 185.

Received 12 December 1986
and accepted 28 January 1987